PROCEEDINGS OF SCIENCE

A measurement of the ratio of light-lepton inclusive semileptonic B decay rates $R(X_{e/\mu}) = \mathcal{B}(B \to Xe\nu) / \mathcal{B}(B \to X\mu\nu)$ using $189\,\mathrm{fb}^{-1}$ of data at Belle II

Henrik Junkerkalefeld[a,*] **on behalf of the Belle II Collaboration**

[a] *Physikalisches Institut, Universität Bonn,*
Nussallee 12, 53115 Bonn, Germany

E-mail: junkerkalefeld@physik.uni-bonn.de

In this work a measurement of the ratio of branching fractions of inclusive semileptonic B meson decays, $R(X_{e/\mu}) = \mathcal{B}(B \to Xe\nu)/\mathcal{B}(B \to X\mu\nu)$ is reported as a probe of $e-\mu$ universality. Electron-positron collisions collected at the $\Upsilon(4S)$ resonance with the Belle II detector corresponding to $189\,\mathrm{fb}^{-1}$ of integrated luminosity are used. One B meson is reconstructed in its fully hadronical decays, while the semileptonic B meson decay is selected by demanding the reconstructed lepton to have a momentum in the B rest frame above $1.3\,\mathrm{GeV}/c$. We find $R(X_{e/\mu}) = 1.033 \pm 0.010 \pm 0.019$. The first contribution to the uncertainty is statistical, the second systematic. This is the most precise branching-fraction based test of $e-\mu$ universality in semileptonic B decays to date and agrees with the Standard Model expectation within $1.3\,\sigma$.

41st International Conference on High Energy physics - ICHEP2022
6-13 July, 2022
Bologna, Italy

*Speaker

PoS(ICHEP2022)745

1. Introduction

Semileptonic B meson decays are a powerful probe of the Standard Model of particle physics (SM). Due to the factorization of the decay process into hadronic and leptonic parts, high precision can be achieved in both theoretical predictions and experimental measurements. By measuring branching fraction ratios of two different lepton types, uncertainties that are associated to common factors like the magnitude of the quark-mixing matrix element $|V_{cb}|$ cancel further.

Any measured deviation from expected values would question lepton universality, a fundamental postulate of the SM that weak interaction couples to the three charged leptons identically. Indeed, this principle has been challenged by combining several measurements of the ratio $R\left(D^{(*)}\right) = \mathcal{B}(B \to D^{(*)}\tau\nu)/\mathcal{B}(B \to D^{(*)}\ell\nu)$, $\ell \in \{e, \mu\}$ [1]. The Belle II detector provides excellent conditions to probe lepton universality in an inclusive way, where the hadronic part of the semileptonic decay is not restricted to certain hadrons in the final states.

In this document such a measurement is presented: the inclusive branching fraction ratio $R(X_{e/\mu}) = \mathcal{B}(B \to Xe\nu)/\mathcal{B}(B \to X\mu\nu)$, using a Belle II collision data set corresponding to an integrated luminosity of 189 fb^{-1}. Natural units are used, specifically $c = 1$.

2. The Belle II detector, collision data and simulated samples

The SuperKEKB accelerator [2] provides asymmetric-energy electron-positron collisions at a center-of-mass (c.m.) energy of $\sqrt{s} = 10.58$ GeV, corresponding to the mass of the $\Upsilon(4S)$ resonance, that almost exclusively decays into a pair of B mesons. The Belle II detector [3, 4] comprises several subsystems and encloses the collider's interaction point in a cylindrical geometry. Closest to the beam pipe is the vertex detector, consisting of several layers of silicon-pixel and silicon-strip detectors. Additionally, a drift chamber (CDC) filled with a gas mixture consisting of C_2H_6 and He in equal parts is used to measure particle tracks. To enable kaon and pion identification, the CDC is surrounded by a Cherenkov-light imaging and time-of-propagation detector in the barrel region and a proximity-focusing, ring-imaging Cherenkov detector in the forward endcap region. Subsequently, the electromagnetic calorimeter (ECL) consists of a barrel and two endcap sections containing CsI(Tl) crystals for the purpose of providing neutral particle and electron identification. It is embedded by a superconducting solenoid that creates a uniform 1.5 T magnetic field along the beam direction. Belle II is concluded by the K_L^0 and muon identification detector, which comprises scintillator strips in the inner part and the endcaps of the barrel and resistive plate chambers in the outer barrel.

The $e^+e^- \to \Upsilon(4S) \to B\bar{B}$ events are modeled using Monte Carlo simulation and contain the signal $B \to X\ell\nu$ events as well as backgrounds arising from hadronic B decays. The `EvtGen` software is used to generate the physics events [5], while the detector simulation is performed with `GEANT4` [6]. The `PHOTOS` software is used to simulate final-state radiation of photons from charged particles [7]. The reconstruction and analysis of simulated events as well as collision data is performed using the open-source Belle II analysis software framework, `basf2` [8].

The inclusive signal model mostly consists of the sum of several resonant decays: $X \in \{D, D^*, D_0^*, D_1, D_1', D_2^*\}$, where the latter four are summarized as D^{**}. The kinematics of $B \to D^{(*)}\,\ell^+\,\nu_\ell$ decays are derived by the BGL [9] form factor model. The modeling of $B \to D^{**}\,\ell^+\,\nu_\ell$

decays is parameterized by BLR [10]. The remaining gap between the measured total B meson decay width [11] and the sum of branching ratios of exclusive decays is filled by non-resonant semileptonic B decays: $X \in \{D^{(*)}\pi\pi, D^{(*)}\eta\}$. They are simulated via intermediate, broad D^{**} resonances using the BLR parametrization.

Backgrounds from e^+e^- continuum processes, i.e., the production of a lighter quark pair $e^+e^- \to q\bar{q}$, $q \in \{c, s, d, u\}$, is modeled by using 18 fb^{-1} of off-resonance collision data, collected 60 MeV below the $\Upsilon(4S)$ resonance.

3. Event reconstruction and selection

To maximize the kinematic control, one B meson, the B_{tag}, is demanded to decay fully hadronically. Its reconstruction is done using the Full Event Interpretation algorithm (`FEI`) [12]. The B_{tag} selection purity is maximized by demanding the beam-constrained mass of the B_{tag}, $M_{\text{bc}} = \sqrt{(\sqrt{s}/2)^2 - |\vec{p}_B^{\,c.m.}|^2}$ to lie within $[5.2725, 5.285]$ GeV. Further, B_{tag} candidates need to obey $\Delta E = (E_B^{c.m.} - \sqrt{s}/2) \in [-0.15, 0.1]$ GeV and the output classifier of the `FEI` algorithm, $\mathcal{P}_{\text{FEI}}$ must be larger than 0.1. This results in a purity of correctly reconstructed B_{tag} candidates of 82 %.

Off-resonant data is scaled by a factor of $c_{\text{off-res}} = (\sqrt{s}_{\text{off-res}}/\sqrt{s}_{\Upsilon(4S)})^2 = 0.989$ to account for the center-of-mass energy dependence in the $e^+e^- \to q\bar{q}$ cross section. Moreover, the B_{tag} properties are scaled by a factor of $1/\sqrt{c_{\text{off-res}}} = 1.006$ to correct for the decreased total event energy in off-resonant collisions. To suppress these continuum events, a boosted decision tree is trained on simulated samples of $B\bar{B}$ decays for signal and continuum events for background, using 21 well-modeled event-shape variables. The threshold on the classifier score is chosen such that 55 % of the continuum is rejected while 97 % of the $B\bar{B}$ events are kept.

After the B_{tag} reconstruction, signal lepton candidates are reconstructed from the remaining tracks. Muon candidates are required to obey $p_T > 0.4$ GeV to reduce the amount of hadrons misidentified as muons. For their identification, the likelihood ratio $\text{PID}_\mu = \mathcal{L}_\mu/(\sum_i \mathcal{L}_i)$, $i \in \{e, \mu, \pi, K, p, d\}$ is utilized, where each particle hypothesis is probed combining information from likelihood functions defined in each sub-detector. The value of PID_μ lies between 1 (very muon-like) to 0 (very background-like) and is demanded to be above 0.95.

Electron candidates are required to have a transverse momentum $p_T > 0.3$ GeV. They are identified by a multiclass boosted decision tree classifier that uses the likelihood ratios from the Belle II sub-systems but additionally utilizes several calorimeter cluster observables. The classifier thresholds are chosen in bins of $(p_\ell^{\text{lab}}, \theta_\ell^{\text{lab}}, q)$ such that a uniform 80% identification efficiency is obtained. The four-momenta of electron candidates are corrected for bremsstrahlung radiation by adding ECL clusters that are found within a lepton momentum dependent distance to the electron track's momentum vector and that are not matched otherwise.

Subsequently, all remaining ECL clusters and tracks are combined in the X system as long as they fulfill certain quality properties to suppress clusters caused by material interactions, beam backgrounds or misidentified tracks. Based on the first particle identification criterion that is fulfilled, the tracks are assigned with a mass hypothesis. The following order (with identification criterion) is applied: electron (same as signal), muons (same as signal), kaons ($\text{PID}_K > 0.6$), protons ($\text{PID}_p > 0.5$), and pions (all remaining tracks).

4. Signal yield determination

The signal yield is determined through a one-dimensional binned maximum-likelihood fit of the lepton momentum in the B_{sig} rest frame, p_ℓ^B. To suppress backgrounds and contributions from $B \to X\tau\nu$ events, $p_\ell^B > 1.3\,\text{GeV}$ is required. In the fit, three templates are defined for the electron and muon channel each: one for the continuum background; one for the collective remaining backgrounds, which are events in which the reconstructed signal lepton candidate either is a true lepton that was mostly created in a secondary decay in the hadronic B decay cascade or a hadron that was misidentified as a lepton; and one template for $B \to X\ell\nu$. Both lepton flavors are fitted simultaneously, so that any correlations between uncertainties affecting both are taken into account.

The $B \to X\ell\nu$ yields are left to float freely in the fit, while the continuum background yields are constrained with a Gaussian term according to the number of events measured in off-resonant data. Additionally, a data-driven Gaussian constraint for the secondary and fake leptons background yields is obtained from a fit to experimental data in dedicated background-enriched control regions where the requirement on the lepton charge and the charge of the B_{tag} inferred from its flavor is reversed, $\Upsilon(4S) \to B^{+,0}_{\text{tag}}, B_{\text{sig}} \to X\ell^+\nu$ + c.c.

The statistical and systematic uncertainties are included into the fit via nuisance parameters, with one parameter per p_ℓ^B bin per template.

5. Systematic uncertainties

The branching fractions of the $B \to D^{(*)}\,\ell^+\,\nu_\ell$ processes are updated to the latest values provided by the HFLAV group [1]. For $B \to D^{**}\,\ell^+\,\nu_\ell$ as well as $B \to D^{(*)}\,\pi\,\pi\,\ell^+\,\nu_\ell$ decays, their total branching fractions are deduced by extrapolating from existing measurements of specific charge configurations to the unobserved final state decays. In all named cases, the results of neutral and charged B mesons are combined assuming isospin symmetry. The branching fractions of the unmeasured $B \to D^{(*)}\,\eta\,\ell^+\,\nu_\ell$ gap modes are assigned a 100 % uncertainty. All branching fraction uncertainties are propagated to the fit in the form of $1\,\sigma$ event weight variations. Shape uncertainties of the fit templates caused by form-factor parameter uncertainties are estimated using the `HAMMER` software package [13]. The resulting p_ℓ^B bin correlations are propagated to the fit as constraints to the nuisance parameters via the sum of the covariance matrices of all individual uncertainty sources.

The lepton identification efficiency and the misidentification probabilities of pions and kaons as leptons in the simulation are corrected using calibration decays reconstructed from experimental data. The corrections are determined as functions of lab-frame momentum, polar angle, and charge of the lepton candidate. The uncertainties in lepton identification efficiencies are propagated via 200 weights that are generated from Gaussian variations using the uncertainties and covariance of the efficiency corrections. For events of a given efficiency or fake rate type falling in the same (p, θ, q) bin, corrections are considered to be fully correlated. For other factors of the same type only the systematic uncertainties are assumed to be correlated.

6. Results and discussion

In Figure 1 the pre- and post-fit distributions of p_ℓ^B for both signal and control regions are presented, depicting the model templates considered in the fit. The electron and muon templates

are fit simultaneously in 10 p_ℓ^B bins each covering a p_ℓ^B range from 1.3 GeV to 2.3 GeV. The last bin of each lepton flavor is extended to account for any higher momenta candidates.

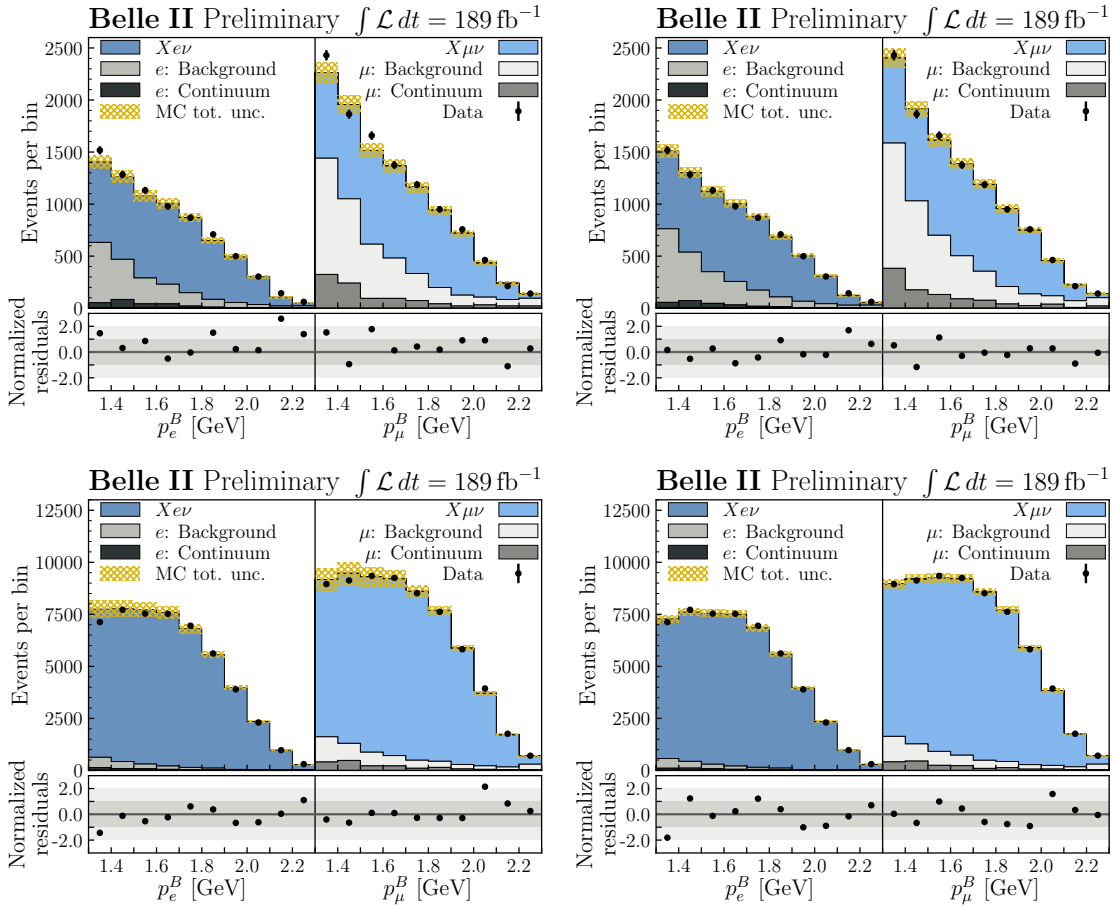

Figure 1: Pre- (left) and post-fit (right) distributions of the lepton momentum in the B_{sig} rest frame, p_ℓ^B, in the incorrect (top) and correct charge (bottom) case. In the pre-fit plots, the normalizations of the combined electron and muon distributions are scaled to the normalizations of the experimental distributions to accommodate any shared efficiency errors that cancel in the $e - \mu$ ratio.

Finally, $R(X_{e/\mu})$ is calculated as

$$R(X_{e/\mu}) = \frac{\epsilon_{X\mu\nu} N_{Xe\nu}}{\epsilon_{Xe\nu} N_{X\mu\nu}} \qquad \text{with} \qquad \epsilon_{X\ell\nu} = \frac{N_{\text{sel}}^\ell f_{B_{\text{tag}}}^{\text{exp./sim.}}}{2 N_{B\bar{B}} \mathcal{B}(B \to X\ell\nu)}, \tag{1}$$

where $N_{B\bar{B}}$ is the number of $B\bar{B}$ events produced in the simulation and N_{sel}^ℓ is the number of $B \to X\ell\nu$ events that pass all selections before the fit. The factor $f_{B_{\text{tag}}}^{\text{exp./sim.}}$ represents the efficiency ratio of the FEI tagging algorithm between experimental and simulated data. Within statistical precision, these factors are found to be consistent between the electron and muon modes and therefore cancel out in the ratio. The efficiencies $\epsilon_{X\ell\nu}$ are calculated with respect to the full phase space and are found to be $\epsilon_{Xe\nu}/f_{B_{\text{tag}}}^{\text{exp./sim.}} = (1.62 \pm 0.03) \times 10^{-3}$ and $\epsilon_{X\mu\nu}/f_{B_{\text{tag}}}^{\text{exp./sim.}} = (2.04 \pm 0.05) \times 10^{-3}$. Uncertainties on N_{sel}^ℓ caused by branching ratio and form factor parameter uncertainties are assumed to be fully correlated across the electron and muon channels.

The impact of each systematic uncertainty on the result is estimated by performing fits to the expected yields of the model templates. Each systematic uncertainty is either included or not, and the resulting uncertainties are compared to the total ones when including all systematics. Assuming that they add up in quadrature, their relative importance can be inferred. The resulting uncertainty values are further validated in studies with generated toy datasets in which the input templates are varied within their uncertainties and the effect on $R(X_{e/\mu})$ is probed.

The largest uncertainties are those associated with lepton identification efficiencies, which account for a relative uncertainty on $R(X_{e/\mu})$ of 1.9 %. Branching fraction and form factor uncertainties mostly cancel out in the $R(X_{e/\mu})$ ratio and therefore hardly contribute (0.1 % and 0.2 %, respectively). Statistical uncertainties are found to be of 1.0 %.

From the fit, the signal yields are extracted to be $N_{Xe\nu} = 48034 \pm 286$ and $N_{X\mu\nu} = 58569 \pm 429$ corresponding to an $R(X_{e/\mu})$ value of

$$R(X_{e/\mu}) = 1.033 \pm 0.010 \pm 0.019 \tag{2}$$

where the first uncertainty is statistical and the second systematic. This result agrees with the Standard Model prediction of 1.006 ± 0.001 [14] within $1.3\,\sigma$ and with a previous measurement from Belle in exclusive $B \to D^{*}\ell\nu$ decays within $0.6\,\sigma$ [15]. So far, the reported result is the most precise test of $e - \mu$ universality in semileptonic B decays based on a branching fraction ratio.

References

[1] Y. Amhis et al. (HFLAV Group), *Eur. Phys. J. C* **81**, 226 (2021)

[2] K. Akai et al. (SuperKEKB accelerator team), *Nucl. Instrum. Meth. A* **907** 188 (2018), arXiv:1809.01958 [physics.acc-ph]

[3] T. Abe et al. (Belle II Collaboration), (2010), arXiv:1011.0352 [physics.ins-det]

[4] W. Altmannshofer et al. (Belle II Collaboration), *Prog. Theor. Exp. Phys.* **2019**, 123C01 (2019)

[5] D. J. Lange, *Nucl. Instrum. Meth. A* **462**, 152 (2001)

[6] S. Agostinelli et al., (GEANT4 Collaboration), *Nucl. Instrum. Meth. A* **506**, 250 (2003)

[7] E. Barberio et al., *Comput. Phys. Commun.* **66**, 115 (1991)

[8] T. Kuhr et al. (Belle II Framework Software Group), *Comput. Softw. Big Sci.* **3**, 1 (2019)

[9] C. Boyd et al., *Phys. Rev. Lett.* **74**, 4603 (1995), arXiv:hep-ph/9412324

[10] F. U. Bernlochner et al., *Phys. Rev. D* **97** 075011 (2018)

[11] P. A. Zyla et al., (Particle Data Group), *Prog. Theor. Exp. Phys.* **2020**, 083C01 (2020)

[12] T. Keck et al., *Comput. Softw. Big Sci.* **3**, 6 (2019), arXiv:1807.08680 [hep-ex]

[13] F. U. Bernlochner et al., *Eur. Phys. J. C* **80**, 883 (2020)

[14] M. Rahimi and K. K. Vos, *JHEP* **11**, 007 (2022), arXiv:2207.03432 [hep-ph]

[15] E. Waheed et al. (Belle Collaboration), *Phys. Rev. D* **100**, 052007 (2019)